HHS Public Access

Author manuscript

Hepatology. Author manuscript; available in PMC 2017 January 01.

Published in final edited form as:

Hepatology. 2016 January ; 63(1): 185–196. doi:10.1002/hep.27927.

Absence of the intestinal microbiota exacerbates hepatobiliary disease in a murine model of primary sclerosing cholangitis

James H. Tabibian[1,2,#], **Steven P. O'Hara**[1,2,#,*], **Christy E. Trussoni**[1,2], **Pamela S. Tietz**[1,2], **Patrick L. Splinter**[1,2], **Taofic Mounajjed**[3], **Lee R. Hagey**[4], and **Nicholas F. LaRusso**[1,2,*]

James H. Tabibian: tabibian.james@mayo.edu; Steven P. O'Hara: ohara.steven@mayo.edu; Christy E. Trussoni: trussoni.christy@mayo.edu; Pamela S. Tietz: tietz.pamela@mayo.edu; Patrick L. Splinter: splinter.patrick@mayo.edu; Taofic Mounajjed: mounajjed.taofic@mayo.edu; Lee R. Hagey: lhagey@ucsd.edu; Nicholas F. LaRusso: larusso.nicholas@mayo.edu

[1]Division of Gastroenterology and Hepatology, Mayo Clinic, Rochester

[2]Center for Cell Signaling in Gastroenterology, Mayo Clinic, Rochester

[3]Division of Anatomic Pathology, Mayo Clinic, Rochester

[4]Division of Gastroenterology, University of California, San Diego, La Jolla

Abstract

Introduction—Primary sclerosing cholangitis (PSC) is a chronic, idiopathic, fibro-inflammatory cholangiopathy. The role of the microbiota in PSC etiopathogenesis may be fundamentally important yet remains obscure. We tested the hypothesis that germ-free (GF) mdr2$^{-/-}$ mice develop a distinct PSC phenotype compared to conventionally-housed (CV) mdr2$^{-/-}$ mice.

Methods—Mdr2$^{-/-}$ mice (n=12) were re-derived as GF by embryo transfer, maintained in isolators, and sacrificed at 60 days in parallel with age-matched CV mdr2$^{-/-}$ mice. Serum biochemistries, gallbladder bile acids, and liver sections were examined. Histologic findings were validated morphometrically, biochemically, and by immunofluorescence microscopy (IFM). Cholangiocyte senescence was assessed by p16^{INK4a} *in situ* hybridization in liver tissue and by β-galactosidase (SA-β-gal) staining in a culture-based model of insult-induced senescence.

Results—Serum biochemistries, including alkaline phosphatase, aspartate aminotransferase, and bilirubin, were significantly higher in GF mdr2$^{-/-}$ ($p<0.01$). Primary bile acids were similar, while secondary bile acids were absent in GF mdr2$^{-/-}$ mice. Fibrosis, ductular reaction, and ductopenia were significantly more severe histopathologically in GF mdr2$^{-/-}$ mice ($p<0.01$) and were confirmed by hepatic morphometry, hydroxyproline assay, and IFM. Cholangiocyte senescence was significantly increased in GF mdr2$^{-/-}$ mice and abrogated *in vitro* by ursodeoxycholic acid treatment.

Conclusions—GF mdr2$^{-/-}$ mice exhibit exacerbated biochemical and histologic features of PSC and increased cholangiocyte senescence, a characteristic and potential mediator of progressive biliary disease. Ursodeoxycholic acid, a commensal microbial metabolite, abrogates senescence *in*

[*]Correspondence: Division of Gastroenterology and Hepatology, Mayo Clinic College of Medicine, 200 First Street, SW, Rochester, MN 55905. larusso.nicholas@mayo.edu and ohara.steven@mayo.edu.

[#]Joint first authors

Disclosures, conflicts of interest: none

vitro. These findings demonstrate the importance of the commensal microbiota and its metabolites in protecting against biliary injury and suggest avenues for future studies of biomarkers and therapeutic interventions in PSC.

Keywords

biliary tract diseases; cholestatic liver disease; biliary epithelial cell; animal models; senescence

INTRODUCTION

Primary sclerosing cholangitis (PSC) is a chronic, cholestatic liver disease characterized by biliary inflammation and periductal fibrosis,[1, 2] a median liver transplantation- (LT) free survival of 12 years,[3] and a predisposition to hepatobiliary carcinogenesis.[4, 5] Despite ongoing research over several decades, significant advances in its medical treatment have not been realized. Given the morbidity and mortality of PSC, lack of established pharmacotherapies,[1, 6, 7] and challenges peri-LT,[8, 9] a better understanding of its etiopathogenesis is critically needed.

PSC is a clinically heterogeneous disease with genetic, immunologic, environmental, and other potential etiopathogenic components.[1, 2, 10] It exhibits remarkable epidemiologic and pathobiological associations with inflammatory bowel disease (IBD). Indeed, IBD (most often ulcerative colitis), a chronic disorder characterized by enteric microbial dysbiosis, [11, 12] is found in approximately 75% of PSC patients. [13, 14]. In addition to and extending these associations is a growing number of studies suggesting that the intestinal microbiota plays an important pathophysiologic role in PSC, hence providing the basis of the “leaky gut” hypothesis.[1, 2] The focus of these studies, though, has been on the deleterious effects of microbial dysbiosis and microbial metabolites in the etiopathogenesis of PSC, and thus the role of the *commensal* (i.e. normal) microbiota, if any, remains unknown.

The multidrug resistance 2 knockout (mdr2$^{-/-}$) mouse is a well-recognized and widely utilized animal model of PSC;[15–17] whether or how the commensal microbiota or its metabolites contribute to its PSC phenotype, however, has not been examined. Therefore, to address this knowledge gap and improve current understanding of the PSC-microbiota relationship, we herein generated the first germ-free (GF) variant of mdr2$^{-/-}$ mice and tested the hypothesis that they develop a distinct hepatobiliary disease phenotype compared to conventionally-housed (CV) mdr2$^{-/-}$ mice. Furthermore, we examined whether GF mdr2$^{-/-}$ mice exhibit differences in cholangiocyte senescence, a characteristic and potentially fundamental mechanism for development and progression of PSC which we recently described,[18] and whether this pathophysiologic cellular state can be abrogated by commensal microbial metabolites. Our collective findings demonstrate significantly exacerbated hepatobiliary disease and increased cholangiocyte senescence in GF mdr2$^{-/-}$ mice and provide proof of concept regarding the protective role of the commensal microbiota and its metabolites in the pathogenesis of biliary injury and PSC.

METHODS

Animal studies

FVB/N background mdr2$^{-/-}$ mice were obtained as a gift from Dr. Oude Elferink (Tytgat Institute, Amsterdam, Netherlands) after obtaining Institutional Animal Care and Use Committee approval. Mice were housed at the Mayo Clinic animal care facility with a 12:12 hour light/dark cycle and ad libitum access to water and standard rodent diet (Purina LabDiet 5053, Richmond, IN). Two F_1 generation breeding pairs were shipped to Taconic (Germantown, NY) for re-derivation as GF mdr2$^{-/-}$ mice by sterile embryo transfer into a pseudopregnant GF surrogate mother. The resultant GF mdr2$^{-/-}$ pups were born and housed in isolators following strict gnotobiotic techniques at Taconic. GF status was validated in accordance with international health monitoring system GF microbiological standards.[19] GF mdr2$^{-/-}$ mice were returned to our facility in vinyl sleeve Taconic GF shipping isolators ventilated with HEPA-filtered air. CV mdr2$^{-/-}$ mice were bred and maintained in parallel at our facility, and both GF and CV mdr2$^{-/-}$ mice, matched on background, age, generation, and male:female ratio, were sacrificed under general anesthesia at 60 days of age. Because mdr2$^{-/-}$ mice typically develop substantial sclerosing cholangitis by this time point, we also examined GF and CV mdr2$^{-/-}$ mice at 30 days of age.[15]

Serum, gallbladder bile, and liver were collected at the time of sacrifice from all mice. Serum liver enzymes, bilirubin, and bile acid concentration were measured by routine clinical chemistry (Marshfield labs, Marshfield, WI). Bile was analyzed by high-pressure liquid chromatography (Hofmann Laboratory, San Diego, CA); conjugated bile acids were quantified in the column effluent by monitoring absorbance at 205 nm (corresponding to the amide bond), and peaks were identified using the relative retention time of standards. The mean hydrophilic-hydrophobic balance (i.e. hydrophobicity index) of bile acids was quantified using a bile salt monomeric hydrophobicity index as previously described.[20] Livers were weighed, snap-frozen or formalin-fixed and paraffin-embedded, and sectioned (4 μm). Sections were stained with hematoxylin and eosin (H&E), Masson's trichrome, or Picrosirius red or utilized for the experiments below.

Given our aim was to investigate the impact of the GF state on disease (PSC) phenotype, not on differences between genotypes, mdr2$^{+/+}$ (WT) mice were not re-derived as GF; CV mdr2$^{+/+}$ mice were used, as needed, as normal controls.

Liver histology

H&E- and trichrome-stained liver sections were examined under light microscopy by a hepatopathologist masked to all mouse data. The following histopathologic features were assessed semi-quantitatively: fibrosis (staged 1–4 by Ludwig criteria), ductular reaction (graded 0–4, with 4 defined as expansion of all portal areas by numerous bile ductular profiles), ductopenia (absence of an interlobular and septal bile duct in >50% of portal tracts), portal inflammation (graded 0–3, with 3 defined as a severe portal inflammatory infiltrate [>50 inflammatory cells/portal tract]), lobular inflammation (graded 0–3, with 3 defined as a severe lobular inflammatory infiltrate [>50 inflammatory cells/high power

field]), and hepatocellular mitoses (present or absent). Ductular reaction and fibrosis were further assessed as described below.

Confocal immunofluorescence microscopy (IFM) and Immunohistochemistry (IHC)

IFM was performed with a Zeiss LSM 510 confocal microscope with a 63x oil objective as previously described.[18] Briefly, unstained liver sections were deparaffinized and rehydrated, boiled in antigen unmasking solution (Vector Laboratories, Burlingame, CA), quenched with Image-iT FX signal enhancer (Life Technologies, Grand Island, NY), and blocked for 1 hour. Slides were then incubated overnight at 4°C with cytokeratin (CK) 19 (goat polyclonal IgG, Santa Cruz Biotechnology, Santa Cruz, CA), CK7 (mouse monoclonal IgG_1, AbCam, Cambridge, MA), alpha-smooth muscle actin (rabbit monoclonal, AbCam), and/or IL-10 and IL-10 receptor (goat polyclonal, Sigma-Aldrich, St. Louis, MO) primary antibodies followed by incubation with corresponding fluorophore-conjugated secondary antibodies (Life Technologies). Coverslips were mounted using ProLong Gold antifade reagent (Life Technologies) with DAPI. For IHC, paraffin embedded tissues were deparaffinized and rehydrated, and boiled in antigen unmasking solution as above. Slides were then incubated overnight at 4°C with CD4 (rabbit polyclonal, Novus Biologicals), CD8 (rabbit monoclonal, Abgent) or anti-neutrophil (rat monoclonal, Cedarlane) primary antibodies followed by incubation with HRP-tagged secondary antibodies and developed using the ImmPACT NovaRed substrate kit (Vector Laboratories).

Morphometric and biochemical assessment of fibrosis

In addition to histologic evaluation of Trichrome-stained liver sections, hepatic fibrosis was confirmed by: **i)** morphometric quantitation of randomly selected fields in Picrosirius red-stained sections using MetaMorph Image Analysis software (Molecular Devices, Sunnyvale, California);[21] **ii)** hepatic hydroxyproline content quantitation using 100 mg frozen liver as previously described;[21, 22] and iii) hepatic alpha-smooth muscle actin expression by IFM as described above.

Fluorescence *in situ* hybridization (FISH)

Expression of $p16^{INK4a}$ mRNA, a well-established marker of cellular senescence, was assessed by FISH as previously described.[18, 23] Briefly, liver section slides were deparaffinized, rehydrated, and boiled in sodium citrate buffer. Slides were prehybridized in a 4X saline-sodium citrate solution containing 3% bovine serum albumin at 55°C and then incubated with $p16^{INK4a}$ LNA probe (Exiqon, Woburn, MA) diluted in hybridization buffer. Slides were hybridized at 55°C for 1 hour and then submitted to a series of decreasing stringency washes. Coverslips were mounted as above. Adobe Photoshop CS3 (Adobe Systems, San Jose, CA) was used to quantitate fluorescence within cholangiocytes.

Cell culture

Normal human cholangiocytes (NHCs)—low passage, well-characterized human biliary epithelial cells[24]—were obtained as a gift from Dr. Juan Medina (University of Navarra, Pamplona, Spain) and utilized in an *in vitro* model of senescence as described recently.[18] Briefly, NHCs were treated with H_2O_2 (50 nM) for 10 days in the presence or absence of

secondary bile acids deoxycholic acid (DCA, 50 μM) and ursodeoxycholic acid (UDCA, 50 μM) or ethanol vehicle (Sigma-Aldrich). Media for each experimental condition were replaced every 48 hours for 10 days, after which senescence-associated β-gal (SA-β-gal) staining was performed (Cell Biolabs, San Diego, CA). The proportion of senescent (i.e. SA-β-gal positive) NHCs was determined for each condition by microscopy of 5 randomly selected areas using a 20x objective as previously described.[18] All experiments were performed in triplicate.

Statistical Analysis

Data were summarized as mean ± standard deviation or as a percentage. Statistical analyses were performed with t-test or Chi-square test for continuous and categorical variables, respectively, using JMP software (SAS Institute, Cary, NC). When assumptions were not met for these tests, Mann-Whitney U or Fisher's exact test were used as appropriate. All tests of significance were two-tailed, and $p < 0.05$ was considered statistically significant.

RESULTS

There were 12 mice in both the GF and CV mdr2$^{-/-}$ mouse groups (i.e. 24 mice total), and 7 of 12 mice in each group were male. Survival in both groups was 100%. There were no differences in gross appearance at the time of sacrifice other than larger cecal size in GF mdr2$^{-/-}$ mice. At a histological level, intestinal tissue revealed typical alterations associated with the GF state, including shallower colonic crypts, decreased ileal villous length, and diminished expression of the epithelial tight junction protein, Zonula occludens 1 (ZO1; Supplementary figure 1). [25, 26] Mean liver weight was similar between groups (1.5 vs. 1.6 grams, respectively, p=0.18).

Serologic evidence of increased cholestasis in GF mdr2$^{-/-}$ mice

We first analyzed serum biochemical markers relevant to hepatobiliary disease. As shown in Figure 1, serum biochemistries, including alkaline phosphatase, aspartate aminotransferase, alanine aminotransferase, bilirubin, and bile acids, were uniformly higher in GF compared to CV mdr2$^{-/-}$ mice, suggestive of more severe disease in the former. This difference was statistically significant in four of these five serum test results (all $p<0.01$), while alanine aminotransferase showed a trend toward significance (p=0.07). We also assessed serum biochemical markers relevant to hepatobiliary disease in younger mice (30 day old), wherein there was a trend toward more severe disease in GF compared to CV mdr2$^{-/-}$ mice (Supplementary Figure 2). Taken together, these findings provide serologic evidence of more severe, progressive cholestasis and hepatobiliary injury in GF compared to CV mdr2$^{-/-}$ mice.

Similar primary bile acid profiles but absence of secondary bile acids in GF mdr2$^{-/-}$ mice

We next assessed bile acids in GF and CV mdr2$^{-/-}$ mouse gallbladder bile. Based on the results of HPLC analyses, we found that there were no significant differences between GF and CV mdr2$^{-/-}$ mice with respect to primary bile acids (Supplementary figure 3A). In addition, there was no significant difference in the average gallbladder bile acid hydrophobicity index between GF and CV mdr2$^{-/-}$ mice (−0.50 vs. −0.44, p=0.12). In

contrast, DCA and UDCA, both secondary bile acids which require bacterial dehydroxylation for their biosynthesis, were undetectable in GF mdr2$^{-/-}$ mice (Supplementary figure 3B), as expected and consistent with the GF state. Therefore, with the exception of the absence of secondary bile acids, GF and CV mdr2$^{-/-}$ mice had similar gallbladder bile profiles and overall hydrophilic-hydrophobic bile acid balance.

Multiple indicators of more advanced hepatic fibrosis in GF mdr2$^{-/-}$ mice

We next examined liver tissue-based parameters of hepatobiliary disease, beginning with fibrosis. Based on blinded histopathologic evaluation of Trichrome-stained liver sections, we found that a significantly higher proportion of GF mdr2$^{-/-}$ mice had advanced (≥ Stage 3) fibrosis (p=<0.001), with four of the GF and none of the CV mdr2$^{-/-}$ exhibiting cirrhosis by 60 days (Figures 2A–C). To validate this finding, we next assessed fibrosis morphometrically in Picrosirius red-stained sections and observed a significantly higher percentage of fibrotic area in GF compared to CV mdr2$^{-/-}$ mice (p=0.016, Figure 2D). We then assessed fibrosis by biochemical measurement of hepatic hydroxyproline concentration and found this to also be significantly higher in GF compared to CV mdr2$^{-/-}$ mice (p=0.035, Figure 2E), indicating more collagen deposition (i.e. fibrosis) in the former. Lastly, using confocal IFM, we evaluated alpha-smooth muscle actin expression and found this to be more prominent in GF compared to CV mdr2$^{-/-}$ mice (Supplementary figure 4A, B), suggesting greater hepatic stellate cell activation, a known driver of hepatic fibrosis. Collectively, these data strongly support the presence of more advanced stage fibrosis in GF compared to CV mdr2$^{-/-}$ mice.

Increased ductular reaction and ductopenia in GF mdr2$^{-/-}$ mice

We next investigated whether there were also differences in other tissue-based features of hepatobiliary disease, namely ductular reaction and ductopenia. Based on histopathologic evaluation of H&E-stained sections, we found more extensive ductular reaction (≥ grade 3) in GF compared to CV mdr2$^{-/-}$ mice (Figures 3A, B); this difference was statistically significant (p=<0.001), with nearly all GF mdr2$^{-/-}$ mice demonstrating grade 4 ductular reaction (Figure 3C). Similarly, ductopenia was also significantly more frequent in GF compared to CV mdr2$^{-/-}$ mice (p=0.004), with all but one GF mdr2$^{-/-}$ mouse demonstrating this finding (Figures 4A–D). We also investigated whether histopathological features of both ductular reaction and ductopenia were present in younger mice (i.e. 30 day old). We found that at this earlier time point, GF mdr2−/− mice had already began to exhibit more severe ductular reaction and more ductopenia compared to CV mdr2−/− mice (Supplementary figure 5).

To validate these findings, we evaluated, using confocal IFM, ductular reaction and ductopenia in CK19-stained liver sections of 60 day old mice. This revealed changes consistent with H&E-based histopathologic evaluation, namely more severe ductular reaction and a higher proportion of ductopenic livers in GF compared to CV mdr2$^{-/-}$ mice (Figures 4E, F). Collectively, these results provide evidence of significantly greater hepatobiliary disease in GF compared to CV mdr2$^{-/-}$ mice, which in general can be detected as early as 30 days post-parturition.

Similar hepatic inflammation and IL-10 expression in GF compared to CV mdr2$^{-/-}$ mice

We next assessed the distribution and degree of hepatic inflammation in GF and CV mdr2$^{-/-}$ mice. Based on histologic evaluation of H&E-stained sections, we did not find significant differences in portal or lobular inflammation at the 30 day or 60 day post-parturition time point or the presence of Councilman bodies, which are associated with hepatocyte injury and inflammation (data not shown). This observation is supported by similar numbers of CD4^{+} cells detected in the portal tracts of both CV and GF mdr2$^{-/-}$ mice by immunohistochemistry (Figures 5A, B); CD8^{+} cells were sparse throughout the liver and showed no difference between CV and GF mdr2$^{-/-}$ mice (Supplementary figure 6). In contrast to lymphocytes, we observed an increase in the number of hepatobiliary neutrophils in GF mice (Figures 5C, D). We next explored hepatic expression of IL-10 (an anti-inflammatory cytokine with hepatoprotective and pro-regenerative properties[27]) and IL-10 receptor in liver sections. Using confocal IFM, we found that there were no differences in expression of IL-10 or its receptor between GF and CV mdr2$^{-/-}$ mice, and in addition, IL-10 receptor was not expressed by cholangiocytes in either condition (data not shown). Therefore, taken together, these results suggest that the more severe disease in GF as compared to CV mdr2$^{-/-}$ mice, at this stage of disease progression, does not appear to be mediated by increased hepatobiliary lymphocyte infiltration or a relative deficiency in IL-10 signaling, but may involve an increased or persistent innate response to tissue injury.

Increased cholangiocyte senescence in GF mdr2$^{-/-}$ mice

In our final set of tissue-based experiments, we began to explore the mechanisms responsible for the more severe disease phenotype in GF compared to CV mdr2$^{-/-}$ mice. Recently, we found cholangiocyte senescence to be a central feature of PSC and a driver of increased pro-fibroinflammatory signaling.[18] Therefore, we next assessed cholangiocyte expression of p16^{INK4a} mRNA, a well-established and specific marker of cellular senescence. Using FISH, we found cholangiocyte p16^{INK4a} expression to be highest in GF mdr2$^{-/-}$ mice (Figures 6A–C); quantitation of cholangiocyte p16^{INK4a} fluorescence intensity confirmed a statistically significant difference (Figure 6D; $p<0.001$), corresponding to the serologic and histologic evidence of increased biliary injury in GF mdr2$^{-/-}$ mice. These data suggest that cholangiocyte senescence is significantly increased in GF compared to CV mdr2$^{-/-}$ mice and may account for the more severe phenotype observed in GF mice.

UDCA, a commensal bacterial metabolite, abrogates cultured cholangiocyte senescence

To further investigate the finding of increased cholangiocyte senescence in GF mdr2$^{-/-}$ mice, in our final set of experiments, we aimed to determine whether bacterial metabolites can protect against injury-induced cholangiocyte senescence and thus account for the less severe hepatobiliary disease seen in CV (compared to GF) mdr2$^{-/-}$ mice. Among the most well-known biliary constituents that depend on bacterial metabolism for their biosynthesis are secondary bile acids; as expected, these were absent in GF mdr2$^{-/-}$ mice. By utilizing a recently developed, *in vitro* model of insult-induced NHC senescence,[18] we tested whether secondary bile acids have cytoprotective effects which might contribute to the less severe phenotype observed in CV compared to GF mdr2$^{-/-}$ mice. Following 10 days of treatment, we found that while DCA exhibited no significant effects, UDCA significantly reduced

NHC senescence (41% reduction, p=0.02) compared to vehicle control (Figures 6E, F). These results suggest that specific commensal bacterial metabolites, including UDCA, are cytoprotective against biliary injury and may thus mediate, at least in part, the differences observed between GF and CV mdr2$^{-/-}$ mice.

DISCUSSION

In this study, we describe, to our knowledge, the first axenic variant of an animal model of PSC, namely the GF mdr2$^{-/-}$ mouse. The major findings here are: **i)** the GF state has unambiguous effects on the features and severity of hepatobiliary disease; **ii)** GF mdr2$^{-/-}$ mice exhibit serologic evidence of increased cholestasis and histologic evidence of increased liver fibrosis, ductular reaction, and ductopenia; **iii)** GF mdr2$^{-/-}$ mice demonstrate a significantly increased proportion of senescent cholangiocytes; and **iv)** UDCA, a product of commensal bacteria which was absent in GF mdr2$^{-/-}$ mice, abrogates insult-induced human cholangiocyte senescence in an *in vitro* model system. These findings may have direct implications for the pathobiology of biliary epithelial injury and the development of novel biomarkers and experimental therapies for PSC.

A growing number of basic, translational, and clinical studies have recently suggested an important etiopathogenic relationship between PSC and the enteric microbiota. For example, the biliary epithelium is exposed to microbial metabolites[28–30] and expresses the receptors (e.g. TLRs) necessary to sense and respond to them.[31] Moreover, in the case of PSC, biliary epithelial cells accumulate bacterial endotoxin[32] and exhibit hypersensitivity to it *in vitro*.[33] These and other supporting data[34, 35] (recently reviewed by the authors elsewhere[36]) have provided rationale for several recent pilot studies of oral antibiotics in patients with PSC, the results of which appear promising.[37] Given, therefore, the prior studies suggesting a detrimental effect of the microbiota in the pathogenesis of PSC, we predicted an attenuated PSC phenotype in the absence of the commensal microbiota in mdr2$^{-/-}$ mice; to our surprise, however, GF mdr2$^{-/-}$ mice exhibited a dramatically worsened PSC phenotype as well as more cholangiocyte senescence.

An evolving concept of progressive tissue injury and fibrosis in chronic liver disease involves increased intestinal permeability and translocation of bacterial molecules and metabolites from the intestinal tract.[38] At a histological level, we observed typical intestinal alterations associated with the GF state, including shallower colonic crypts, decreased ileal villous length, and diminished expression of the epithelial tight junction protein, ZO1 (Supplementary figure 1). While these data suggest diminished intestinal tight junction integrity, this likely did not contribute to the more severe phenotype in the GF mouse as no microbial products were present in the GF state, and in the absence of an inciting injury, GF mice are not known to demonstrate a hepatic disease phenotype. However, the more severe phenotype observed in our GF animals is congruent with recent observations demonstrating more severe hepatic injury, including fibrosis, in GF C57BL/6 mice treated with the hepatotoxins carbon tetrachloride or thioacetamide.[39] Intriguingly, in this same study, a similar severe phenotype was observed in MyD88/TRIF-deficient animals exposed to these hepatotoxins, suggesting that the lack of innate immune signaling can indeed enhance hepatic injury. Hence, taken together, these data indicate a significant

beneficial role of commensal microbiota in preventing or mitigating insult-induced hepatic injury.

These novel observations are of particular intrigue in the context of the aforementioned data regarding the PSC-microbiota relationship and the potentially critical role of cholangiocyte senescence in the pathogenesis of PSC.[18] Collectively, these findings suggest that while microbial dysbiosis may initiate biliary injury and ultimately induce chronic biliary disease (i.e. PSC), the commensal microbiota may have a protective effect against biliary injury and disease, as summarized in a working conceptual model in Figure 7. Although still an active area of research, the protective effects of the commensal microbiota can be considered in two broad categories: **i)** production of cytoprotective metabolites (or decreased production of injurious metabolites);[40–42] and **ii)** facilitation of normal immunologic development.[42]

Regarding the first category, we found that GF mdr2$^{-/-}$ mice not only exhibit evidence of significantly greater cholestasis, ductular reaction, ductopenia, and fibrosis, but also cholangiocyte p16^{INK4a} expression, a well-established marker of cellular senescence. Moreover, we found that UDCA, a secondary bile acid known to require commensal bacterial metabolism for its biosynthesis exhibits an anti-senescent effect in an *in vitro* model of insult-induced cholangiocyte senescence. These two findings, which may be interrelated, are relevant given senescent cells can transition to a potentially pathologic state referred to as a senescence-associated secretory phenotype (SASP).[18, 43, 44] SASP cells, in turn, can alter their microenvironment, reinforce the senescent phenotype (e.g. induce senescence in neighboring cells), and initiate pro-fibroinflammatory and pro-tumorigenic cellular responses and outcomes.[43, 45, 46] Therefore, we propose that the high proportion of senescent cholangiocytes observed in GF mdr2$^{-/-}$ mice represents both a marker as well as a driver of more severe hepatobiliary disease (e.g. ductopenia, fibrosis), and that UDCA may be a cytoprotective, anti-senescent commensal microbial metabolite. Intriguingly, previous reports have demonstrated that UDCA feeding in MDR2$^{-/-}$ mouse, when started immediately after weaning improved fibrosis and inflammation.[47] However, UDCA feeding started later (2 month-old mice), when fibroobliteration is present, induced bile infarcts and exacerbated the disease phenotype.[48] Whether improved inflammation and fibrosis in UDCA fed mice correlates with diminished senescence in this model remains to be determined. We do acknowledge, however, that UDCA has not been clearly shown to improve outcomes in patients with PSC, although this may be due to several other factors, including: **i)** the heterogeneity of PSC, **ii)** the presence of/need for other cytoprotective commensal microbial metabolites (as UDCA alone reduced senescence induction by only 41%), and/or **iii)** UDCA initiation too late in the course of disease (i.e. after cholangiocyte senescence has already been established).

Regarding the second category of protective effects of the commensal microbiota, we did not find differences in the lymphocytic response, e.g. increased hepatic CD4^{+} lymphocyte infiltrates or decreased expression of the anti-inflammatory cytokine IL-10, in GF compared to CV mdr2$^{-/-}$ mice to account for the more severe disease observed in the former. However, a contribution by functional or other immunologic differences cannot be ruled out. Indeed, while histological examination revealed a similar inflammatory response between GF and CV mdr2$^{-/-}$ mice, our IHC data demonstrated increased neutrophils in the GF livers.

Whether and how this persistent innate immune response contributes to a more severe phenotype is an area of active investigation. Moreover, we acknowledge that numerous microbial metabolites may influence hepatobiliary responses to injury via proper development and differentiation of T-cell subsets. Hence, differences in hepatic lymphocyte cell subsets may influence hepatobiliary response to injury and is also an active area of investigation. With this in mind, it is plausible that an alternative potential explanation for the increased degree of cholangiocyte senescence in GF mdr2$^{-/-}$ mice might be a relative immunologic defect in GF mdr2$^{-/-}$ mice resulting in impaired clearance of senescent biliary epithelial cells.[49, 50] Senescent cell clearance has only recently been explored but may ultimately hold therapeutic promise in PSC (even in more advanced stages of disease) and other disorders.[44]

In summary, by generating the first GF variant of the mdr2$^{-/-}$ murine model of PSC, we have demonstrated that the absence of the commensal microbiota leads to more severe biliary injury and increased cholangiocyte senescence, a potentially key marker of and mechanism for progressive biliary injury in PSC. Moreover, we have shown that UDCA, a commensal microbial metabolite which was absent in GF mice, abrogates cholangiocyte senescence in an *in vitro* model of insult-induced senescence. These findings provide proof of concept regarding the protective role of the commensal microbiota and its metabolites in the pathobiology of biliary injury and PSC. Therefore, future studies should aim to better understand the structure and role of the commensal microbiota in PSC and identify other commensal microbial metabolites which may impart cytoprotective effects against biliary injury. Insights from such studies may generate new knowledge regarding how to harness the therapeutic properties of the commensal microbiota for translation into potential therapies for PSC.

Supplementary Material

Refer to Web version on PubMed Central for supplementary material.

Acknowledgments

This work was supported by National Institutes of Health Grants AI089713 (to S.P.O.), DK57993 (to N.F.L), the Mayo Foundation, PSC Partners Seeking a Cure, and the Clinical and Optical Microscopy Cores of the Mayo Clinic Center for Cell Signaling in Gastroenterology (P30DK084567).

The authors would like to thank Dr. Alan Hofmann at the University of California, San Diego, for his expert insights regarding bile acid analyses and our study findings, Dr. Purna Kashyap for his input regarding GF mouse investigations, and Dr. Douglas Simonetto in the laboratory of Dr. Vijay Shah for his assistance with hydroxyproline quantitation.

Abbreviations

CK	cytokeratin
CV	conventionally-housed
GF	germ-free
IFM	immunofluorescence microscopy

LPS	lipopolysaccharide
LT	liver transplantation
PRR	pathogen recognition receptors
PSC	primary sclerosing cholangitis
SASP	senescence-associated secretory phenotype
TLR	toll-like receptor

References

1. Tabibian JH, Lindor KD. Primary sclerosing cholangitis: a review and update on therapeutic developments. Expert Rev Gastroenterol Hepatol. 2013; 7:103–114. [PubMed: 23363260]
2. Weismuller TJ, Wedemeyer J, Kubicka S, Strassburg CP, Manns MP. The challenges in primary sclerosing cholangitis--aetiopathogenesis, autoimmunity, management and malignancy. J Hepatol. 2008; 48 (Suppl 1):S38–57. [PubMed: 18304683]
3. Farrant JM, Hayllar KM, Wilkinson ML, Karani J, Portmann BC, Westaby D, et al. Natural history and prognostic variables in primary sclerosing cholangitis. Gastroenterology. 1991; 100:1710–1717. [PubMed: 1850376]
4. Tabibian JH, Lindor KD. Challenges of Cholangiocarcinoma Detection in Patients with Primary Sclerosing Cholangitis. Journal of Analytical Oncology. 2012; 1:50–55.
5. Bangarulingam SY, Bjornsson E, Enders F, Barr Fritcher EG, Gores G, Halling KC, et al. Long-term outcomes of positive fluorescence in situ hybridization tests in primary sclerosing cholangitis. Hepatology. 2010; 51:174–180. [PubMed: 19877179]
6. Chapman R, Fevery J, Kalloo A, Nagorney DM, Boberg KM, Shneider B, et al. Diagnosis and management of primary sclerosing cholangitis. Hepatology. 2010; 51:660–678. [PubMed: 20101749]
7. Beuers U, Boberg KM, Chapman RW, Chazouillères O, Invernizzi P, Jones DE, et al. EASL Clinical Practice Guidelines: management of cholestatic liver diseases. J Hepatol. 2009; 51:237–267. [PubMed: 19501929]
8. Brandsaeter B, Friman S, Broome U, Isoniemi H, Olausson M, Backman L, et al. Outcome following liver transplantation for primary sclerosing cholangitis in the Nordic countries. Scand J Gastroenterol. 2003; 38:1176–1183. [PubMed: 14686722]
9. Ali JM, Bonomo L, Brais R, Griffiths WJ, Lomas DJ, Huguet EL, et al. Outcomes and diagnostic challenges posed by incidental cholangiocarcinoma after liver transplantation. Transplantation. 2011; 91:1392–1397. [PubMed: 21516065]
10. Levy C, Lindor KD. Primary sclerosing cholangitis: epidemiology, natural history, and prognosis. Semin Liver Dis. 2006; 26:22–30. [PubMed: 16496230]
11. DuPont AW, DuPont HL. The intestinal microbiota and chronic disorders of the gut. Nat Rev Gastroenterol Hepatol. 2011; 8:523–531. [PubMed: 21844910]
12. Duboc H, Rajca S, Rainteau D, Benarous D, Maubert MA, Quervain E, et al. Connecting dysbiosis, bile-acid dysmetabolism and gut inflammation in inflammatory bowel diseases. Gut. 2013; 62:531–539. [PubMed: 22993202]
13. Ngu JH, Gearry RB, Wright AJ, Stedman CA. Inflammatory bowel disease is associated with poor outcomes of patients with primary sclerosing cholangitis. Clin Gastroenterol Hepatol. 2011; 9:1092–1097. quiz e1135. [PubMed: 21893134]
14. Wiesner RH, LaRusso NF. Clinicopathologic features of the syndrome of primary sclerosing cholangitis. Gastroenterology. 1980; 79:200–206. [PubMed: 7399227]
15. Fickert P, Fuchsbichler A, Wagner M, Zollner G, Kaser A, Tilg H, et al. Regurgitation of bile acids from leaky bile ducts causes sclerosing cholangitis in Mdr2 (Abcb4) knockout mice. Gastroenterology. 2004; 127:261–274. [PubMed: 15236191]

16. Tabibian JH, Macura SI, O'Hara SP, Fidler JL, Glockner JF, Takahashi N, et al. Micro-computed tomography and nuclear magnetic resonance imaging for noninvasive, live-mouse cholangiography. Lab Invest. 2013; 93:733–743. [PubMed: 23588707]
17. Smit JJ, Schinkel AH, Oude Elferink RP, Groen AK, Wagenaar E, van Deemter L, et al. Homozygous disruption of the murine mdr2 P-glycoprotein gene leads to a complete absence of phospholipid from bile and to liver disease. Cell. 1993; 75:451–462. [PubMed: 8106172]
18. Tabibian JH, O'Hara SP, Splinter PL, Trussoni CE, Larusso NF. Cholangiocyte senescence via N-Ras activation is a characteristic of primary sclerosing cholangitis. Hepatology. 2014
19. Taconic Animal Health Standards. Germ-free mice. 2013. [Internet][cited 2014 Jan 7]. Available from: http://www.taconic.com/user-assets/Documents/Quality/Health_Standards_2pgs.pdf
20. Heuman DM, Hylemon PB, Vlahcevic ZR. Regulation of bile acid synthesis. III. Correlation between biliary bile salt hydrophobicity index and the activities of enzymes regulating cholesterol and bile acid synthesis in the rat. J Lipid Res. 1989; 30:1161–1171. [PubMed: 2769071]
21. Yamaguchi K, Yang L, McCall S, Huang J, Yu XX, Pandey SK, et al. Inhibiting triglyceride synthesis improves hepatic steatosis but exacerbates liver damage and fibrosis in obese mice with nonalcoholic steatohepatitis. Hepatology. 2007; 45:1366–1374. [PubMed: 17476695]
22. Bona S, Filippin LI, Di Naso FC, de David C, Valiatti B, Isoppo Schaun M, et al. Effect of antioxidant treatment on fibrogenesis in rats with carbon tetrachloride-induced cirrhosis. ISRN Gastroenterol. 2012; 2012:762920. [PubMed: 22577570]
23. de Planell-Saguer M, Rodicio MC, Mourelatos Z. Rapid in situ codetection of noncoding RNAs and proteins in cells and formalin-fixed paraffin-embedded tissue sections without protease treatment. Nat Protoc. 2010; 5:1061–1073. [PubMed: 20539282]
24. Banales JM, Saez E, Uriz M, Sarvide S, Urribarri AD, Splinter P, et al. Up-regulation of microRNA 506 leads to decreased Cl−/HCO3− anion exchanger 2 expression in biliary epithelium of patients with primary biliary cirrhosis. Hepatology. 2012; 56:687–697. [PubMed: 22383162]
25. Abrams GD, Bauer H, Sprinz H. Influence of the normal flora on mucosal morphology and cellular renewal in the ileum. A comparison of germ-free and conventional mice. Lab Invest. 1963; 12:355–364. [PubMed: 14010768]
26. Ukena SN, Singh A, Dringenberg U, Engelhardt R, Seidler U, Hansen W, et al. Probiotic Escherichia coli Nissle 1917 inhibits leaky gut by enhancing mucosal integrity. PLoS One. 2007; 2:e1308. [PubMed: 18074031]
27. Louis H, Van Laethem JL, Wu W, Quertinmont E, Degraef C, Van den Berg K, et al. Interleukin-10 controls neutrophilic infiltration, hepatocyte proliferation, and liver fibrosis induced by carbon tetrachloride in mice. Hepatology. 1998; 28:1607–1615. [PubMed: 9828225]
28. Pohl J, Ring A, Stremmel W, Stiehl A. The role of dominant stenoses in bacterial infections of bile ducts in primary sclerosing cholangitis. Eur J Gastroenterol Hepatol. 2006; 18:69–74. [PubMed: 16357622]
29. Olsson R, Bjornsson E, Backman L, Friman S, Hockerstedt K, Kaijser B, et al. Bile duct bacterial isolates in primary sclerosing cholangitis: a study of explanted livers. J Hepatol. 1998; 28:426–432. [PubMed: 9551680]
30. Hiramatsu K, Harada K, Tsuneyama K, Sasaki M, Fujita S, Hashimoto T, et al. Amplification and sequence analysis of partial bacterial 16S ribosomal RNA gene in gallbladder bile from patients with primary biliary cirrhosis. J Hepatol. 2000; 33:9–18. [PubMed: 10905580]
31. Chen XM, O'Hara SP, Nelson JB, Splinter PL, Small AJ, Tietz PS, et al. Multiple TLRs are expressed in human cholangiocytes and mediate host epithelial defense responses to Cryptosporidium parvum via activation of NF-kappaB. J Immunol. 2005; 175:7447–7456. [PubMed: 16301652]
32. Sasatomi K, Noguchi K, Sakisaka S, Sata M, Tanikawa K. Abnormal accumulation of endotoxin in biliary epithelial cells in primary biliary cirrhosis and primary sclerosing cholangitis. J Hepatol. 1998; 29:409–416. [PubMed: 9764987]
33. Mueller T, Beutler C, Pico AH, Shibolet O, Pratt DS, Pascher A, et al. Enhanced innate immune responsiveness and intolerance to intestinal endotoxins in human biliary epithelial cells contributes to chronic cholangitis. Liver Int. 2011; 31:1574–1588. [PubMed: 22093333]

34. Lichtman SN, Keku J, Clark RL, Schwab JH, Sartor RB. Biliary tract disease in rats with experimental small bowel bacterial overgrowth. Hepatology. 1991; 13:766–772. [PubMed: 2010172]
35. Yamada S, Ishii M, Liang LS, Yamamoto T, Toyota T. Small duct cholangitis induced by N-formyl L-methionine L-leucine L-tyrosine in rats. J Gastroenterol. 1994; 29:631–636. [PubMed: 8000512]
36. Tabibian JH, Talwalkar JA, Lindor KD. Role of the microbiota and antibiotics in primary sclerosing cholangitis. Biomed Res Int. 2013; 2013:389537. [PubMed: 24232746]
37. Tabibian JH, Weeding E, Jorgensen RA, Petz JL, Keach JC, Talwalkar JA, et al. Randomised clinical trial: vancomycin or metronidazole in patients with primary sclerosing cholangitis - a pilot study. Aliment Pharmacol Ther. 2013; 37:604–612. [PubMed: 23384404]
38. Cesaro C, Tiso A, Del Prete A, Cariello R, Tuccillo C, Cotticelli G, et al. Gut microbiota and probiotics in chronic liver diseases. Dig Liver Dis. 2011; 43:431–438. [PubMed: 21163715]
39. Mazagova M, Wang L, Anfora AT, Wissmueller M, Lesley SA, Miyamoto Y, et al. Commensal microbiota is hepatoprotective and prevents liver fibrosis in mice. Faseb J. 2015; 29:1043–1055. [PubMed: 25466902]
40. Rakoff-Nahoum S, Paglino J, Eslami-Varzaneh F, Edberg S, Medzhitov R. Recognition of commensal microflora by toll-like receptors is required for intestinal homeostasis. Cell. 2004; 118:229–241. [PubMed: 15260992]
41. Olszak T, An D, Zeissig S, Vera MP, Richter J, Franke A, et al. Microbial exposure during early life has persistent effects on natural killer T cell function. Science. 2012; 336:489–493. [PubMed: 22442383]
42. Hooper LV, Littman DR, Macpherson AJ. Interactions between the microbiota and the immune system. Science. 2012; 336:1268–1273. [PubMed: 22674334]
43. Burton DG. Cellular senescence, ageing and disease. Age (Dordr). 2009; 31:1–9. [PubMed: 19234764]
44. Tchkonia T, Zhu Y, van Deursen J, Campisi J, Kirkland JL. Cellular senescence and the senescent secretory phenotype: therapeutic opportunities. J Clin Invest. 2013; 123:966–972. [PubMed: 23454759]
45. Coppe JP, Patil CK, Rodier F, Sun Y, Munoz DP, Goldstein J, et al. Senescence-associated secretory phenotypes reveal cell-nonautonomous functions of oncogenic RAS and the p53 tumor suppressor. PLoS Biol. 2008; 6:2853–2868. [PubMed: 19053174]
46. Acosta JC, O'Loghlen A, Banito A, Guijarro MV, Augert A, Raguz S, et al. Chemokine signaling via the CXCR2 receptor reinforces senescence. Cell. 2008; 133:1006–1018. [PubMed: 18555777]
47. Van Nieuwkerk CM, Elferink RP, Groen AK, Ottenhoff R, Tytgat GN, Dingemans KP, et al. Effects of Ursodeoxycholate and cholate feeding on liver disease in FVB mice with a disrupted mdr2 P-glycoprotein gene. Gastroenterology. 1996; 111:165–171. [PubMed: 8698195]
48. Fickert P, Zollner G, Fuchsbichler A, Stumptner C, Weiglein AH, Lammert F, et al. Ursodeoxycholic acid aggravates bile infarcts in bile duct-ligated and Mdr2 knockout mice via disruption of cholangioles. Gastroenterology. 2002; 123:1238–1251. [PubMed: 12360485]
49. Xue W, Zender L, Miething C, Dickins RA, Hernando E, Krizhanovsky V, et al. Senescence and tumour clearance is triggered by p53 restoration in murine liver carcinomas. Nature. 2007; 445:656–660. [PubMed: 17251933]
50. Kang TW, Yevsa T, Woller N, Hoenicke L, Wuestefeld T, Dauch D, et al. Senescence surveillance of pre-malignant hepatocytes limits liver cancer development. Nature. 2011; 479:547–551. [PubMed: 22080947]

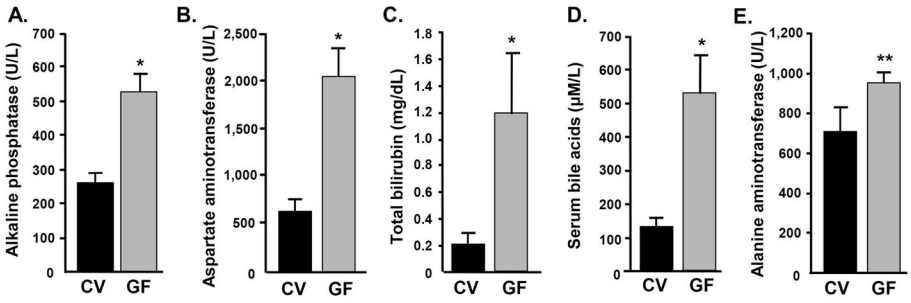

Figure 1.

Germ-free (GF) mdr2$^{-/-}$ mice have significantly more severe serum biochemical abnormalities. Serum A) alkaline phosphatase, B) aspartate aminotransferase, C) bilirubin, and D) bile acids, are all significantly higher in GF compared to CV mdr2$^{-/-}$ mice (*$p<0.001$), and E) alanine aminotransferase shows a trend toward being significantly higher in GF mdr2$^{-/-}$ mice (**$p=0.07$). These differences are indicative of more severe hepatobiliary disease in GF mdr2$^{-/-}$ mice.

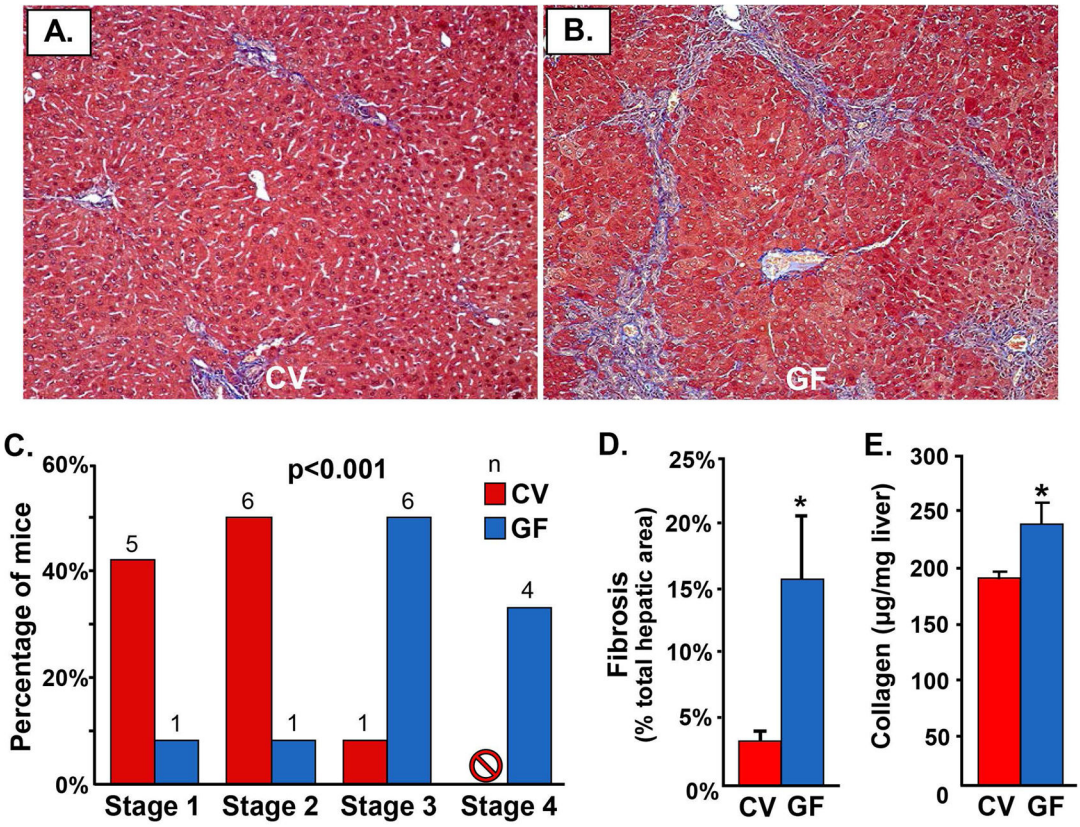

Figure 2.

Germ-free (GF) mdr2$^{-/-}$ mice demonstrate more hepatic fibrosis histologically, morphometrically, and biochemically. Representative images of Masson's Trichrome-stained liver sections of A) CV mdr2$^{-/-}$ and B) GF mdr2$^{-/-}$ mice. C) Based on histopathologic evaluation of Trichrome-stained liver sections, a significantly higher proportion of GF compared to CV mdr2$^{-/-}$ mice exhibit advanced fibrosis (≥ Stage 3) by 60 days ($p<0.001$). D) Morphometric assessment of Picrosirius red-stained liver sections demonstrates a significantly higher percentage of fibrotic area in GF compared to CV mdr2$^{-/-}$ mice ($p=0.016$). E) Biochemical assessment of hepatic fibrosis confirms significantly increased hydroxyproline concentration in GF compared to CV mdr2$^{-/-}$ mice ($p=0.035$). Taken together, these data provide multimodal evidence of more advanced hepatic fibrosis in GF mdr2$^{-/-}$ mice.

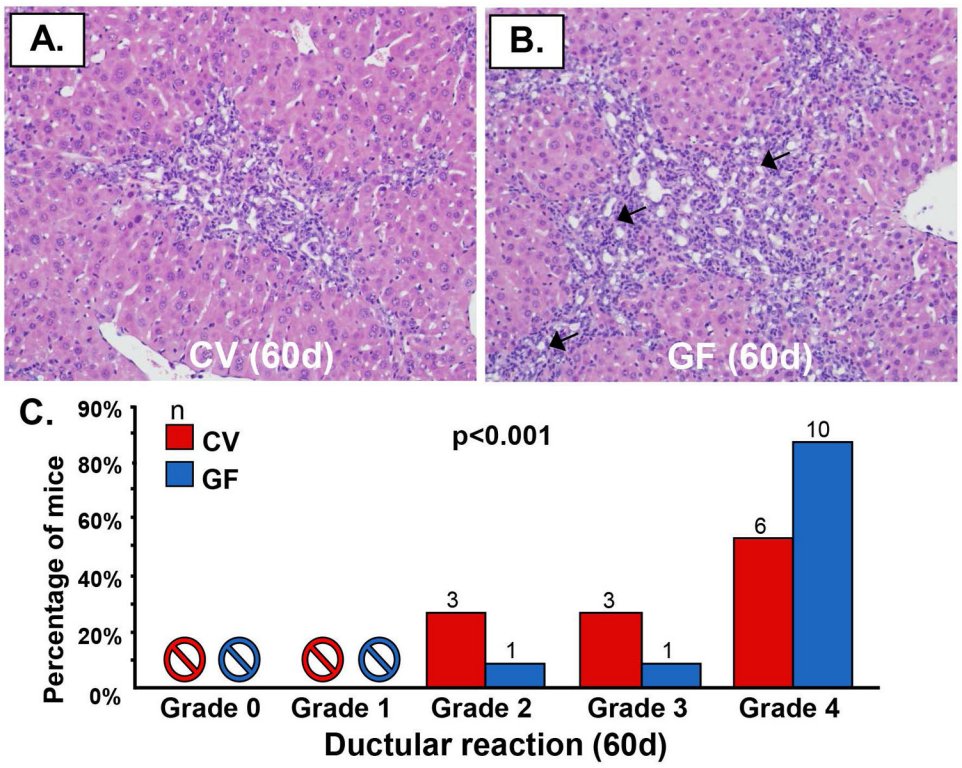

Figure 3.

Germ-free (GF) mdr2$^{-/-}$ mice exhibit significantly more ductular reaction. Representative images of H&E-stained liver sections of A) CV mdr2$^{-/-}$ and B) GF mdr2$^{-/-}$ mice showing periportal regions and ductular reaction. C) Based on histopathologic evaluation, there appears to be significantly more ductular reaction (arrows) in GF compared to CV mdr2$^{-/-}$ mice ($p<0.001$), with all but two GF mdr2$^{-/-}$ mice demonstrating grade 4 ductular reaction, an indicator of severe biliary injury.

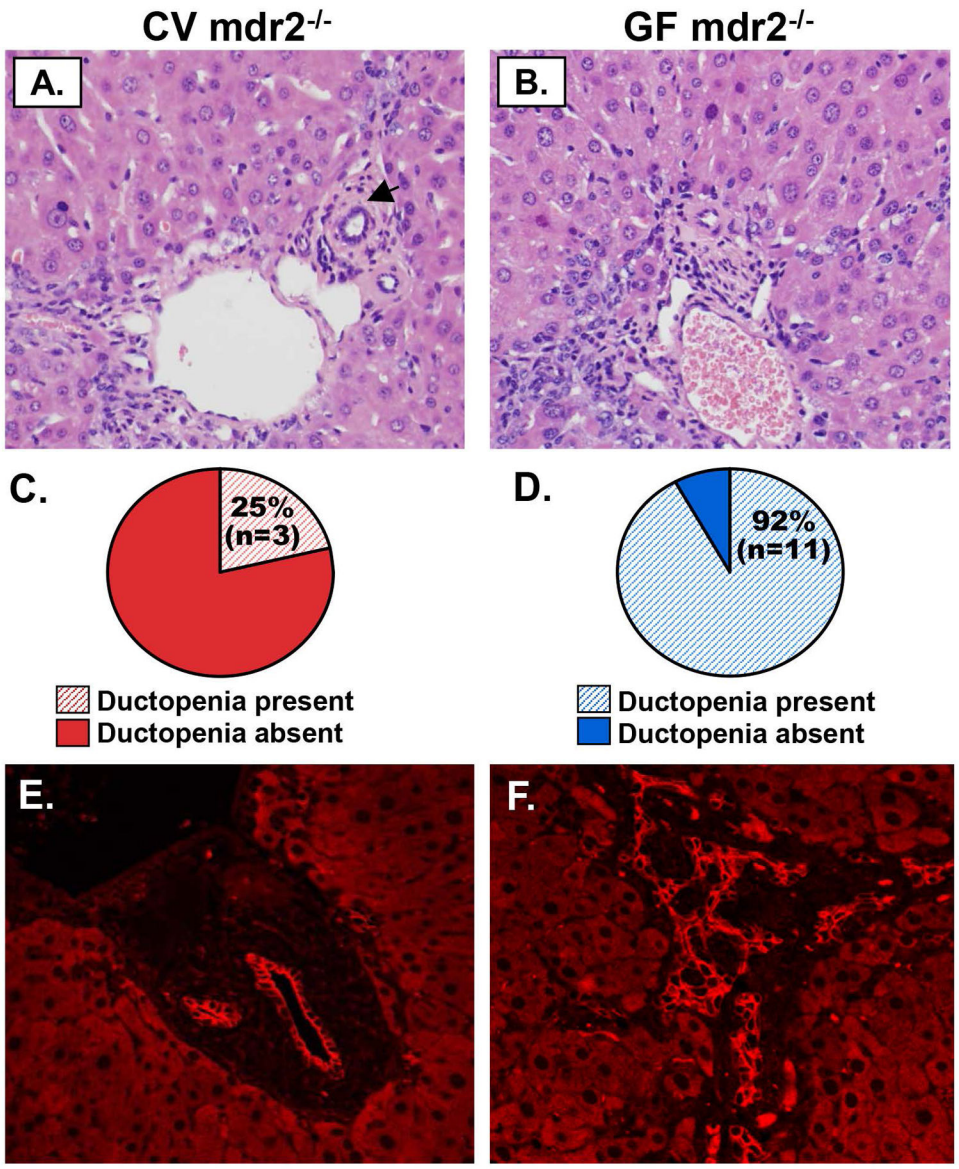

Figure 4.

Germ-free (GF) mdr2$^{-/-}$ mice demonstrate significantly more ductopenia by light microscopy and confocal immunofluorescence microscopy (IFM). Representative light microscopy images of H&E-stained A) CV mdr2$^{-/-}$ and B) GF mdr2$^{-/-}$ mouse liver sections; black arrowheads denote bile duct branches (absent in GF mdr2$^{-/-}$ mouse liver image). Histopathologic evaluation of C) CV and D) GF mdr2$^{-/-}$ liver sections reveals a significantly greater proportion of ductopenia in GF mdr2$^{-/-}$ mice (p=0.004), with all but one being ductopenic. E & F. IFM of CK-19 (red) of mouse liver sections confirms markedly increased ductular reaction and ductopenia in GF compared to CV mdr2$^{-/-}$ mice.

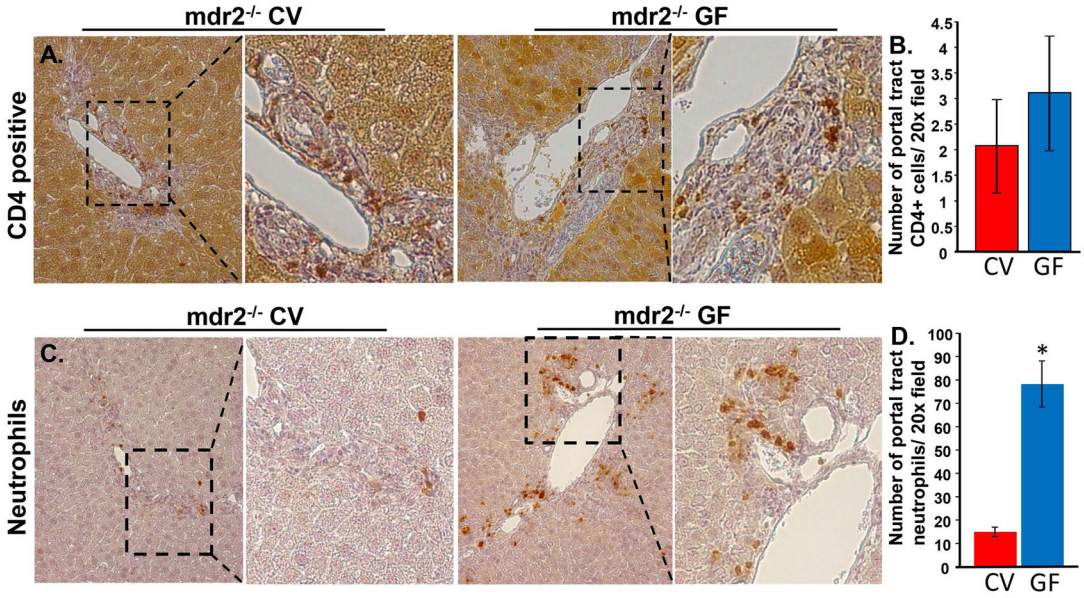

Figure 5.

$CD4^+$ T-cells are present in CV and GF $mdr2^{-/-}$ mice, while GF mice exhibit significantly increased numbers of neutrophils. A. Representative light microscope images of IHC for $CD4^+$ T-cells in CV and GF $mdr2^{-/-}$ mice. $CD4^+$ cells accumulated in portal tracts of both groups of mice. B. Quantitative analysis (5 mice per group, 10 portal tracts per mouse liver) demonstrated similar numbers of $CD4^+$ cells/20x field. C. Representative light microscope images of IHC for neutrophils. The neutrophils also aggregated in portal tracts in both CV and GF $mdr2^{-/-}$ mice. D. Quantitative analysis demonstrated increased numbers of neutrophils in the GF $mdr2^{-/-}$ mice (*, $p< 0.001$).

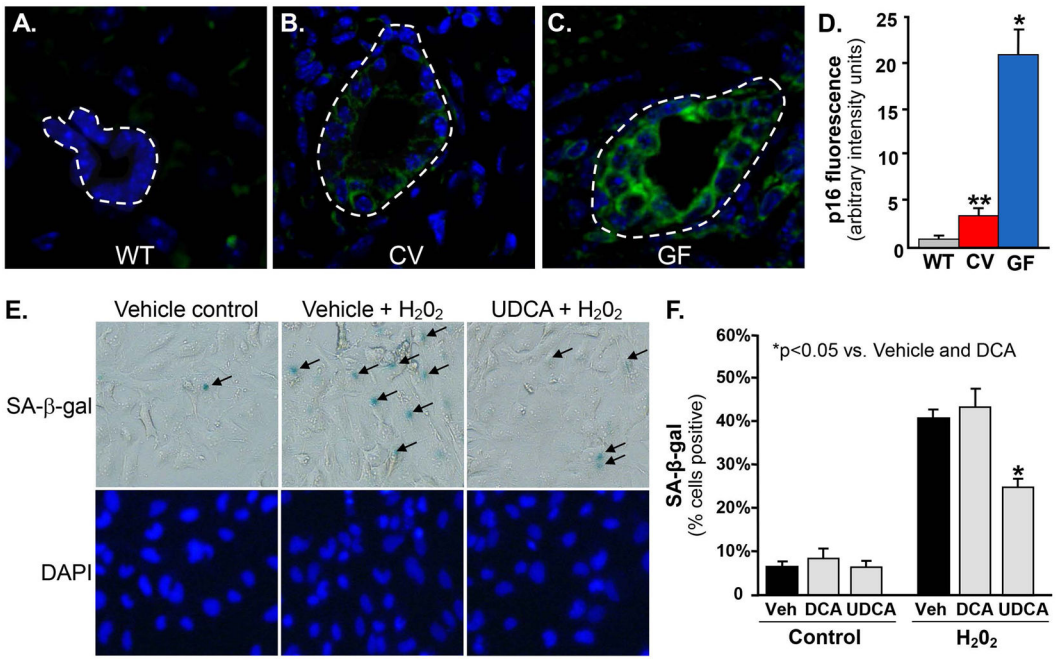

Figure 6.

Cholangiocyte senescence is increased in germ-free (GF) mdr2$^{-/-}$ mice and can be abrogated *in vitro* by the commensal bacterial metabolite, ursodeoxycholic acid. Representative images of A) WT, B) CV mdr2$^{-/-}$, and C) GF mdr2$^{-/-}$ mouse liver p16^{INK4a} FISH, a well-established marker of cellular senescence used in tissue section assessment (p16^{INK4a}, green; DAPI, blue). D. Quantitation p16^{INK4a} fluorescence intensity demonstrates significantly more cholangiocyte senescence in GF mdr2$^{-/-}$ mice than both CV mdr2$^{-/-}$ and WT mice ($p<0.001$). E. *In vitro* model of cholangiocyte senescence (exposure to 50 nM H_20_2, a known inducer of cellular senescence) demonstrates that secondary bile acids (known metabolites of commensal bacteria) can protect against cholangiocyte injury and senescence. Cells were treated every 48 hours with or without deoxycholic acid (DCA), ursodeoxycholic acid (UDCA), or ethanol vehicle (Veh). Representative bright field and fluorescence microscopy images following 10 days of treatment demonstrating increased SA-β-gal stain (blue) positivity (black arrows), a well-established *in vitro* marker of cellular senescence. **F.** Quantitation of SA-β-gal stain-positive cells demonstrates that treatment with UDCA, but not DCA, results in significant abrogation of H_20_2-induced NHC senescence (41% reduction, $p=0.02$).

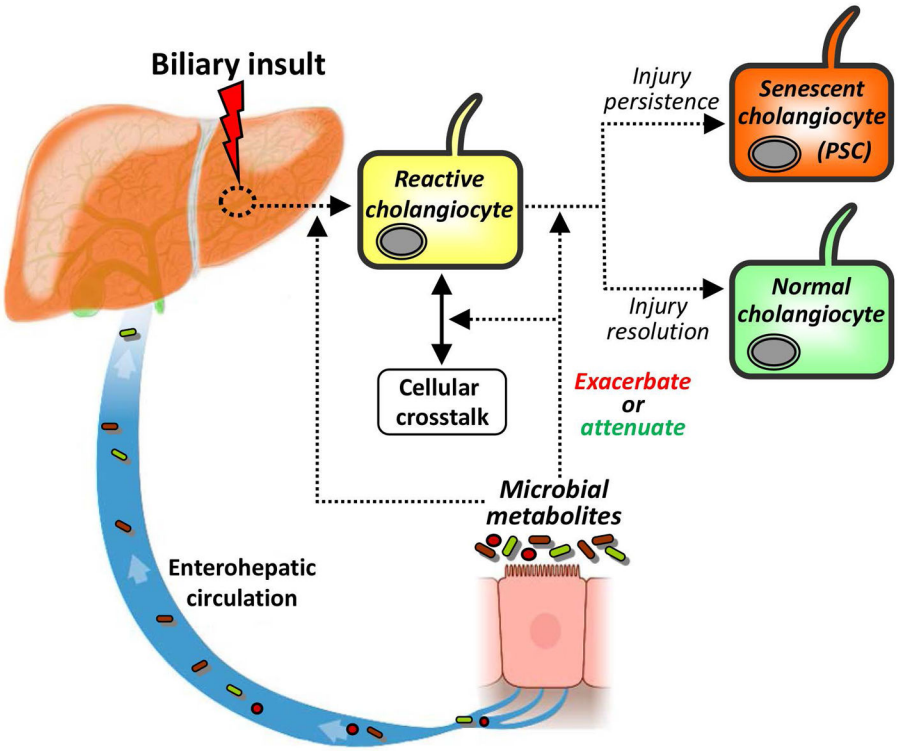

Figure 7.

Conceptual framework for the role of the microbiota in the etiopathogenesis of PSC. In this working model, the cholangiocyte is exposed to a biliary insult, to which it responds through increased expression of proinflammatory mediators and induction of epithelial repair processes (e.g. proliferation), i.e. a phenotype known as the reactive cholangiocyte. Intricate cellular crosstalk between resident and recruited hepatobiliary cells, including hepatocytes, progenitor cells, fibroblasts, leukocytes, and/or cholangiocytes themselves, is subsequently increased in an attempt to resolve biliary injury. The dynamics and outcomes of these signaling processes are modified by and depend on the composition of the microbiota and its metabolites. In the setting of inadequate cytoprotective commensal microbial metabolites (coupled with host immunogenetic susceptibility), there is impaired resolution of biliary injury and consequent progression to chronic hepatobiliary disease. Chronic hepatobiliary disease, most notably PSC, is characterized and may be driven by increased cholangiocyte senescence, a pathobiologial cellular phenotype which can progress to a state of hypersecretion of pro-fiboinflammatory and oncogenic mediators known as the senescence-associated secretory phenotype (SASP). The SASP may be associated may lead to the clinico-pathologic sequelae of PSC, including liver failure and cholangiocarcinoma, and is an area of ongoing investigation.